



1 Reactive Organic Carbon Air Emissions from Mobile Sources in the 2 United States

3 Benjamin N. Murphy^{1*}, Darrell Sonntag², Karl M. Seltzer³, Haval O. T. Pye¹, Christine Allen⁴,
4 Evan Murray⁵, Claudia Toro⁵, Drew R. Gentner⁶, Cheng Huang⁷, Shantanu Jathar⁸, Li Li⁶,
5 Andrew A. May⁹, and Allen L. Robinson¹⁰

6 ¹Center for Environmental Measurement and Modeling, US Environmental Protection Agency, Research Triangle
7 Park, North Carolina 27711, United States

8 ²Department of Civil and Construction Engineering, Brigham Young University, Provo, Utah 84602, United States

9 ³Office of Air quality Planning and Standards, US Environmental Protection Agency, Research Triangle Park, North
10 Carolina 27711, United States

11 ⁴General Dynamics Information Technology, 79 T.W. Alexander Drive, Research Triangle Park, NC 27709, United
12 States

13 ⁵Office of Transportation and Air Quality, US Environmental Protection Agency, Ann Arbor, Michigan 48105, United
14 States

15 ⁶Department of Chemical and Environmental Engineering, Yale University, New Haven, CT 06511, United States

16 ⁷State Environmental Protection Key Laboratory of Cause and Prevention of Urban Air Pollution Complex, Shanghai
17 Academy of Environmental Sciences, Shanghai, 200233, China

18 ⁸Department of Mechanical Engineering, Colorado State University, Fort Collins, Colorado 80523, United States

19 ⁹Department of Civil, Environmental and Geodetic Engineering, Ohio State University, Columbus, Ohio 43210,
20 United States

21 ¹⁰Department of Mechanical Engineering, Carnegie Mellon University, Pittsburgh, Pennsylvania 15213, United
22 States; Carnegie Mellon University Africa, BP 6150 Kigali, Rwanda

23 *Correspondence to: Benjamin N. Murphy (murphy.ben@epa.gov)

24 **Abstract:** Mobile sources are responsible for a substantial controllable portion of the reactive organic carbon (ROC)
25 emitted to the atmosphere, especially in urban environments of the United States (U.S.). We update existing methods
26 for calculating mobile source organic particle and vapor emissions in the U.S. with over a decade of laboratory data
27 that parameterize the volatility and organic aerosol (OA) potential of emissions from onroad vehicles, nonroad
28 engines, aircraft, marine vessels, and locomotives. We find that existing emission factor information from teflon filters
29 combined with quartz filters collapses into simple relationships and can be used to reconstruct the complete volatility
30 distribution of ROC emissions. This new approach consists of source-specific filter artifact corrections and state-of-
31 the-science speciation including explicit intermediate volatility organic compounds (IVOCs), yielding the first
32 bottom-up volatility-resolved inventory of U.S. mobile source emissions. Using the Community Multiscale Air
33 Quality model, we estimate mobile sources account for 20-25% of the IVOC concentrations and 4.4-21.4% of ambient
34 OA. The updated emissions and air quality model reduce biases in predicting fine-particle organic carbon in winter,
35 spring, and autumn throughout the U.S. (4.3-11.3% reduction in normalized bias). We identify key uncertain
36 parameters that align with current state-of-the-art research measurement challenges.

37 1. Introduction

38 Ambient particulate matter (PM) and ozone (O₃) have detrimental impacts on human health and the environment (U.S.
39 EPA, 2019, 2020c; Pye et al., 2021) with disparate impacts across societal groups (Tessum et al., 2021). Non-methane
40 organic gases (NMOG) are precursors to PM and O₃, and reducing NMOG could reduce criteria pollutants and their
41 associated mortality throughout the United States (U.S.) (Pye et al., 2022a). Mobile source emissions continue to be
42 a major contributor to modern anthropogenic NMOG emissions. In contrast to other NMOG sources such as
43 vegetation, mobile emissions have been reduced through successful regulatory policy and the introduction of cleaner
44 engine and control technologies (Lurmann et al., 2015; Gentner et al., 2017; Winkler et al., 2018; Bessagnet et al.,



45 2022). Yet, effective management of urban and regional air quality still depends on accurate and detailed
46 characterization of the carbon-containing compounds emitted by mobile sources.

47 Fossil-fuel combustion emissions comprise thousands of organic compounds with widely varying volatility,
48 depending on source type (Drozd et al., 2018; Lu et al., 2018). The lowest volatility compounds are emitted principally
49 in the particle phase and are typically classified as primary organic aerosol (POA). Conventionally this portion of
50 emissions is sampled using filters which are weighed or processed off-line with thermal-optical techniques, solvent
51 extraction, and other methodologies (Chow et al., 1993; Birch and Cary, 1996; U.S. EPA, 2022b). The highest
52 volatility NMOGs are emitted in the gas-phase and enhance O₃ formation when oxidized in the atmosphere, a process
53 that also enhances PM mass via secondary organic aerosol (SOA) formation. U. S. EPA emission tools like the MOTO
54 Vehicle Emission Simulator (MOVES) (U.S. EPA, 2020b) and the SPECIATE database (U.S. EPA, 2020a) provide
55 emission estimates and speciation for POA (assumed to be nonvolatile) and NMOGs. The ‘Conventional’ path in Fig.
56 1 depicts this process. However, laboratory and field measurement campaigns have demonstrated that much of the
57 mobile source POA is subject to gas-particle partitioning and filter sampling artifacts, semivolatile, which complicates
58 the interpretation of filter-based measurements (Robinson et al., 2010; Bessagnet et al., 2022). These compounds
59 principally include (Table 1) semivolatile organic compounds (SVOCs) and intermediate volatility organic
60 compounds (IVOCs), with IVOCs being key contributors to filter artifacts (May et al., 2013a, b). Accurately
61 representing SVOCs and IVOCs is important because they are SOA precursors and are underestimated in
62 contemporary models and emission databases (Gentner et al., 2012; Tkacik et al., 2012; Zhao et al., 2014; Zhao et al.,
63 2015, 2016b).

64 Some air quality models (AQMs) have incorporated semivolatile organic compounds (SVOCs) and IVOCs by
65 adapting emissions inputs either with a data pre-processing step or during the AQM runtime (Murphy and Pandis,
66 2009; Shrivastava et al., 2011; Ahmadov et al., 2012; Bergström et al., 2012; Koo et al., 2014; Woody et al., 2015;
67 Zhao et al., 2016a; Woody et al., 2016; Jathar et al., 2017b; Murphy et al., 2017). However, these approaches rely on
68 broad application of assumptions that may not be appropriate for specific source types since sampling artifacts will
69 bias low-emitting and high-emitting sources differently (Robinson et al., 2010). As emissions from individual
70 combustion sources are continually reduced in response to tightening regulations, accounting for these potential biases
71 becomes important. Bottom-up approaches are needed that revise emission factors and speciation profiles for
72 individual source types. Datasets like this exist for some areas like Europe (Manavi and Pandis, 2022), Japan (Morino
73 et al., 2022) and China (Chang et al., 2022).

74 This paper documents the transition of U. S. EPA mobile emission tools from the conventional paradigm that considers
75 operationally defined particulate organic matter (OM) and NMOG emission factors and speciation to one that
76 accommodates the full complexity of atmospheric carbon-containing trace pollutants. To accomplish this, we consider
77 total Reactive Organic Carbon (ROC), defined by Saffedine et al. (2017) and Heald and Kroll (2020) as all reactive
78 organic compound mass across gas and particle phases excluding methane. We catalogue updates to 51 diverse mobile
79 source categories across multiple categories and engine, fuel, and control types. Further, we demonstrate procedures
80 for integrating existing inventory emission factors with state-of-the-art chemical composition measurements, pointing



81 out where critical uncertainties could be further resolved in the future. Finally, we document the impact the updates
82 have on source-specific and sector-wide emissions as well as regional-scale pollutant formation and transport
83 predicted by an updated version (2020) of the Community Multiscale Air Quality (CMAQ) regional-scale AQM.

84 **2. Materials and Methods**

85 **2.1 Mobile Emission Modeling**

86 To develop the new framework and estimate potential impacts from speciation updates, we used existing estimates for
87 2016 annual mobile emissions for the contiguous U.S. We considered five categories including onroad, nonroad, air,
88 rail, and marine. The MOVES3 model predicts emissions for onroad and nonroad sources using county-level fleet
89 properties and activity data. The dominant U.S. onroad vehicle sources are light-duty gasoline cars and trucks and
90 heavy-duty diesel trucks. Nonroad emission sources include construction, agricultural, and lawn equipment as well as
91 nonroad recreational vehicles. The Aviation Environmental Design Tool (AEDT), maintained by the Federal Aviation
92 Administration, predicts landing, taxi, and take-off emissions for aircraft and emissions from ground support
93 equipment (Faa, 2022). Rail emissions are calculated using confidential line-haul activity data that were summarized
94 at the county-level, while rail-yard emissions are based on supply fuel use and yard switcher counts provided by
95 companies (U.S. EPA, 2022a). Marine emissions include both port and underway conditions for large, generally
96 international ships, vessels, and smaller boats operating near shore (U.S. EPA, 2022a). The MOVES3 model predicts
97 emissions from recreational boats as part of the nonroad recreational equipment category.

98 We also collected national total annual fuel usage data for each source from the models to calculate an effective fuel-
99 based OM emission factor (see section S1). These effective emission factors range from 1-20 mg (kg-fuel)⁻¹ for the
100 newest gasoline, diesel, and compressed natural gas (CNG) vehicles to over 6000 mg (kg-fuel)⁻¹ for nonroad gasoline
101 two-stroke engines. In the process of reviewing each mobile source OM emission rate, we discovered and corrected
102 several minor errors and limitations to compressed natural gas sources and uncontrolled nonroad diesel exhaust (see
103 section S2).

104 **2.2 Reactive Organic Carbon (ROC)**

105 To accurately simulate the behavior of mobile emissions, we must consider total ROC which includes organic carbon
106 (OC) and non-carbon mass from compounds from the most volatile species like ethane and formaldehyde to
107 chemically complex, high molecular weight compounds (e.g. oligomers) (Heald and Kroll, 2020). Conventional
108 metrics for reporting OM and NMOG are operationally defined based on measurement methods and conditions;
109 therefore, they are difficult to compare across tests and among other ROC sources. Furthermore, uncertainties are
110 introduced when they are speciated with profiles measured at different conditions. To improve standardization, we
111 introduce two new metrics: CROC (condensable reactive organic carbon) and GROC (gaseous reactive organic
112 carbon). CROC is defined as compounds with saturation concentration (C^*) less than 320 $\mu\text{g m}^{-3}$ (Table 1), with this
113 boundary corresponding to *n*-alkanes with 20±1 carbon atoms. CROC includes SVOCs ($0.32 < C^* \leq 320 \mu\text{g m}^{-3}$) and
114 low volatility organic compounds (LVOCs; $C^* \leq 0.32 \mu\text{g m}^{-3}$). Whereas, GROC is defined as the sum of compounds
115 with C^* greater than 320 $\mu\text{g m}^{-3}$ corresponding to IVOCs ($320 < C^* \leq 3.2 \times 10^6 \mu\text{g m}^{-3}$) and volatile organic compounds
116 (VOCs; $C^* > 3.2 \times 10^6 \mu\text{g m}^{-3}$) (Donahue et al., 2009; Murphy et al., 2014). CROC and GROC align with well-known



117 categories in the volatility basis set (VBS) space, so they may be applied straight-forwardly to speciation profiles in
118 recent literature containing both explicit compounds and lumped groups.

119 We apply a two-step methodology to process gas- and particle-phase emissions ('ROC' path in Fig. 1). First, we
120 estimate total GROC and CROC emissions from existing NMOG and OM emission factors, respectively, while
121 considering measurement uncertainties like sampling setup losses (e.g. tubing) and filter artifacts. We then speciate
122 GROC and CROC using state-of-the-science profiles. For GROC, these include explicit IVOC compounds where
123 available and lumped IVOC groups distinguished by their saturation concentration and functionality. The
124 methodology for processing CROC emissions similarly uses volatility profiles from recent literature.

125 **2.2.1 GROC Emissions and Speciation**

126 Total NMOG emissions are measured from mobile emissions by combining total hydrocarbons (THC) with carbonyl
127 compounds and subtracting methane (see section S3) (Kishan et al., 2006; May et al., 2014). Lu et al. (2018) compiled
128 measurements for onroad vehicles, nonroad equipment, and an aircraft turbine engine. That study concluded that
129 methods using heated sampling and a heated flame-ionization detector (FID) can capture both IVOCs and VOCs, but
130 that speciation methods like canister or tedlar bag sampling analyzed with gas-chromatography-FID miss essentially
131 all IVOCs due to wall losses to the sampling materials. Assuming that NMOG emission rates are based on heated FID
132 sampling, we set GROC emission rates equal to total NMOG emission rates across all sources, and we speciated
133 GROC emissions using profiles that include VOCs and IVOCs.

134 Many studies have reported speciated organic gases normalized to total IVOC or VOC (Lu et al., 2018; Jathar et al.,
135 2017a; Zhao et al., 2015, 2016b; Huang et al., 2018; Drozd et al., 2018). A key parameter used to integrate these data
136 is the IVOC/NMOG ratio (see section S4), which ranges from ~4.6% for gasoline vehicle cold start exhaust to 67%
137 for marine residual oil. Gasoline fuel evaporation profiles of GROC were assumed to be the same as NMOG since
138 IVOCs are not expected to contribute substantially to those emissions (Gentner et al., 2012). The profile for whole
139 diesel fuel evaporation was updated to be consistent with fuel characterization in Gentner et al. (2012) (see Section
140 S1c). SPECIATEv5.1 contains thousands of explicit species and many mixtures of compounds (e.g. oils, unspciated
141 terpenes, etc.) reported by previous studies. Recent studies have constrained the unknown portion of IVOCs and VOCs
142 with lumped groups resolved by volatility and often by structure/functionality features (e.g. branched, cyclic,
143 oxygenated, etc.). We leverage the representative compound structures in SPECIATE developed by Pye et al. (2022b)
144 to classify these emissions by functional groups, and their subsequent atmospheric chemistry. Table S2 summarizes
145 the new IVOC profiles. Species-based ozone and OA potential were calculated for each emission source using
146 relationships from Seltzer et al., (2021) which were expanded by Pye et al. (2022b)

147 **2.2.2 CROC Emissions and Speciation**

148 We estimate effective OM emission factors using the MOVES-predicted national total OM emissions normalized to
149 the total fuel usage for each source (see section S1). The MOVES model relies on conventional measurements of total
150 PM emissions sampled and weighed on Teflon filters. The SPECIATE database, meanwhile, stores the weight percent
151 of OC measured by thermal optical techniques from samples collected on quartz filters (U.S. EPA, 2022b) normalized
152 by coincident bulk PM measurements from the Teflon filter (see section S5). SPECIATE also applies a source-



153 dependent OM/OC factor to adjust for non-carbon organic mass (i.e. hydrogen, oxygen), which represents OM once
 154 added to OC (Table S1a) (Reff et al., 2009; Simon et al., 2011). Previous studies have demonstrated that OM emission
 155 factors vary with changing temperature and OM loading (Lipsky and Robinson, 2006; Robinson et al., 2010; May et
 156 al., 2013b, a; Jathar et al., 2020). AQMs that take this behavior into account typically distribute OM emissions among
 157 volatility bins using reference distributions. May et al. (2013b, a) constrained parameters for calculating volatility-
 158 resolved emissions assuming OC is measured on a quartz filter. Although this approach performs well for average
 159 cases, it is less accurate when applied to sources that are low or high emitting, for which absorptive partitioning biases
 160 are more substantial (Fig. 2). For an exceedingly low-emitting source (low OM loading), SVOC emissions that would
 161 normally partition to the particle phase under ambient conditions could go undetected as they pass through the filter.

162 Additionally, reported OM emissions are sometimes artifact-corrected using a secondary quartz filter behind the
 163 Teflon filter sample, which allows for adsorbed SVOCs and IVOCs to be neglected. Because these corrections are not
 164 uniformly applied across all studies, May et al. (2013b, a) reported reference volatility profiles assuming OM emission
 165 factors had not been adsorptive-artifact corrected. Yet this is not always applicable for the emission rates informing
 166 MOVES and must be resolved at the source level based on the underlying emission data. To address both adsorptive
 167 and absorptive partitioning biases, we apply CROC/OM parameterizations developed from detailed measurement data
 168 and informed by filter-based OM emission factors (see section S6) (May et al., 2013b, a; Huang et al., 2018; Jathar et
 169 al., 2020). The method accounts for filter artifact corrections by adding missing SVOC emissions for low OM-loading
 170 tests and neglecting IVOCs and higher-volatility SVOCs that would be captured on the front filter during high OM-
 171 loading tests. The CROC/OM parameterization for onroad gasoline is based on data from 64 vehicles and so is more
 172 robust than the parameterization for onroad heavy-duty diesel with particulate filters (DPF), which is based on 3
 173 vehicles (Section S7), or the aircraft engine parameterization, which is based on one sample. More work is needed to
 174 better constrain the CROC/OM parameters.

175 The impact of this new approach for translating inventory OM emissions is shown in Fig. 2. We use the onroad
 176 gasoline light-duty cold start volatility profile in Table S5 to estimate the effective ambient organic aerosol emission
 177 factor at 298 K and C_{OA} equal to $10 \mu\text{g m}^{-3}$ given a filter-based OM emission factor in mg kg^{-1} fuel. Also shown are
 178 trends using parameters reported by Robinson et al (2007) and Lu et al. (2020), which have been used in contemporary
 179 air quality models. The filter-based OM emission factor (EF_{OM}) is multiplied by the volatility distribution, and VBS
 180 partitioning theory (Eq. 1) is used to calculate the effective ambient OA emission factor ($EF_{OM,Amb}$):

$$181 \quad EF_{OM,Amb} = EF_{OM} \sum_{i=1}^{n_{tot}} \frac{\alpha_i}{1 + C_i^*/10} \quad (1)$$

182 where n_{tot} is the number of volatility parameters in the vector α . The ‘Lu et al.’ and ‘Robinson et al.’ lines are directly
 183 proportional to the nonvolatile emission factor because they do not consider nonlinear dependence on the filter-based
 184 OM emission factor. Meanwhile, the ROC approach enhances emissions at low emission factors (to correct for SVOC
 185 breakthrough) and reduces them at high emission factors (to remove IVOCs partitioning to the filter). Also shown on
 186 Fig. 2 are filter-based OM emission factors for PreTier 2, Tier 2 (2001-2004), and Tier 2 (2004+) vehicles, which
 187 exhibit emissions reductions with newer standards. For the older vehicles, the ‘Lu et al.’ and ‘Robinson et al.’



188 approaches give similar estimates for effective ambient OM as the new approach, but as emission factors decrease,
189 those methods may overpredict evaporation and underpredict the particle emission factors. At the lowest OM emission
190 factors, even using the nonvolatile approach may underpredict effective ambient OA emission factors because
191 significant SVOCs could have broken through the filter and should be considered for ambient partitioning.

192 We did not adjust GROC emissions in response to CROC/OM conversion, but the sum of total ROC emissions for
193 each source does not change substantially from the sum of NMOG and OM (Fig. S22). We then updated existing
194 SPECIATE profiles with volatility distributions of LVOCs and SVOCs normalized to CROC (Table S5a). Because
195 data on the functionality of these low volatility emissions is lacking, we assume they share similar chemical properties
196 (i.e. reactivity) to linear alkanes as a proxy for more complex mixtures of aliphatics and other compounds.

197 **2.3 Air Quality Model Configuration**

198 We used an updated version of the Community Multiscale Air Quality (CMAQ) model v5.3.2 to quantify the impact
199 of the new mobile emissions on regional-scale air quality (U.S. EPA, 2021; Appel et al., 2021). Hourly ambient air
200 concentrations of OA and O₃ were simulated for the entire year 2017 at 12 km horizontal resolution with inputs from
201 EPA's air QUALity Time Series (EQUATES) project (U.S. EPA, 2022c; Foley et al., 2023). Meteorology was
202 simulated with WRFv4.1.1. The Biogenic Emission Inventory System (BEIS) predicted biogenic gas emissions online
203 in CMAQv5.3.2. Gas- and aerosol-phase chemistry are modeled with the Carbon Bond 6 mechanism (CB6r3_AE7)
204 with updates for production of SOA from mobile IVOCs implemented by Lu et al. (2020) Anthropogenic emissions
205 are described in the US EPA 2017 emission platform technical science document and EQUATES documentation (U.S.
206 EPA, 2022a, c). Mobile emissions for 2017 were recalculated in order to update speciation and apply both
207 IVOC/NMOG and CROC/OM adjustments. The 'CMAQ-ROC' simulation implements all revisions to mobile
208 elemental carbon (EC) speciation described in section S2 and the methods described in sections 2.2.1 and 2.2.2. The
209 EC speciation updates result in substantial changes to nonroad diesel, aircraft, marine and rail source (Table S9).
210 Because MOVES uses source- and species-specific emission rates for HAPs rather than relying on generic speciation
211 of NMOG, ROC updates for HAPs are not propagated to the air quality model simulations, although we show potential
212 changes to national-scale HAP emissions from updates to VOC speciation. Volatile chemical product (VCP) emissions
213 are simulated for 2017 with the VCPy tool (Seltzer et al., 2021). Nonoxygenated and oxygenated IVOC emissions
214 from VCPs are represented with the IVOC chemistry from Lu et al. (2020), which results in an average SOA yield of
215 approximately 30% at ambient conditions across all IVOCs. However, Pennington et al. (2021) found the oxygenated
216 IVOC SOA yield to be 6.28%, though this yield warrants re-evaluation with better speciation and yield data given the
217 diverse mix of oxygenated IVOCs with varying molecule functionalities that can influence SOA production (Humes
218 et al., 2022). Based on available information, we reduce the CMAQ-predicted VCP SOA concentrations by 33.8% to
219 account for the overrepresentation of SOA from VCP oxygenated IVOCs (see section S7).

220 We assess model performance for O₃ and OC during the 2017 model year with aily-averaged measurements at routine
221 monitoring sites. We also perform a separate CMAQ simulation for comparison that is consistent with the EQUATES
222 project, which assumes the speciation of OM emissions from all sources are consistent with the volatility distribution
223 of a small diesel generator (Robinson et al., 2007). This 'EQUATES' simulation also utilizes the simplified potential-



224 combustion SOA (pcSOA) approach used in publicly available versions of CMAQ (Murphy et al., 2017). The CMAQ-
225 ROC simulation neglects pcSOA since the role of mobile and VCP IVOC SOA formation are explicitly accounted
226 for. Finally, we also analyzed two simulations with mobile and VCP SOA precursors each set to zero to quantify direct
227 sector contributions to total OA. This approach does not account for the contributions these sectors make to the
228 atmospheric oxidant capacity through emissions of low molecular weight VOCs and nitrogen oxides.

229 3. Results and Discussion

230 3.1 Volatility-Resolved Mobile Source ROC Emissions

231 Using the 2016 annual predictions from MOVES and the other mobile emission models processed and speciated with
232 the ‘ROC’ approach, we explore for the first time a complete bottom-up inventory of organic carbon emissions from
233 mobile sources in the U.S. Figure 1 shows the results of the ROC and Conventional approaches for one example
234 source, onroad heavy-duty diesel equipped with particulate filters. Non-organic particulate matter species such as ions
235 and other PM are equivalent in both approaches. Nonvolatile OM emissions in the Conventional approach are
236 distributed in the ROC approach to a range of SVOCs and IVOCs, which are predominantly alkanes and branched
237 compounds for diesel sources. The magnitude of emission factors for compounds in the VOC volatility range from
238 onroad diesel sources are reduced by 47.8% due to the introduction of IVOCs (IVOC/GROC = 52.2%), and the
239 distribution of VOC functionality is changed substantially due to adoption of VOC speciation profiles from Lu et al.
240 (2018). Unknown ROC mass is also reduced from 7% of total emissions to 0.7% after introducing IVOCs. Emission
241 factors vary by orders of magnitude across mobile sources, motivating careful accounting of sampling biases (Figs.
242 S18-S21), which requires the ROC approach in the emission modeling workflow to be complex and involve multiple
243 tools and intermediate steps (Fig. S1).

244 Figure 3 shows the predicted contributions of source types and functional groups across the volatility spectrum for
245 2016 ROC inventory. The VOC emissions are roughly evenly distributed between onroad and nonroad sources (1130
246 and 1045 kt yr⁻¹, respectively), IVOCs are weighted towards onroad (62%), and CROC (i.e. SVOCs and larger
247 compounds) is roughly split among onroad, nonroad, and others. Tailpipe (i.e. exhaust) emissions while running
248 represent the majority across all volatility categories (56% of total ROC), although evaporative sources are important
249 in the VOC range (38%), and similar to prior estimates (Gentner et al., 2009). It could be counter-intuitive, given
250 laboratory data on start and idle emission factors, that the start/idle operating mode does not contribute more to total
251 ROC emissions. This result could be due in part to substantially more time spent by sources in the running mode
252 during normal operation, but it could also be partly due to MOVES neglecting start modes for nonroad sources. Drozd
253 et al. (2018) found that cold start IVOC fuel-based emission factors are about 6 times larger than those from hot-
254 running-start emissions for newer vehicles, which is consistent with the post Tier 2 gasoline vehicles in this work. For
255 older vehicles though, the ROC inventory predicts greater IVOC emissions factors for hot-running modes than cold-
256 start for older vehicles (Table S1a and Table 2). Further research is needed to constrain NMOG emission factors and
257 IVOC/NMOG ratios for older (pre-2004) vehicles that are expected to have contributed approximately 72% of onroad
258 gasoline ROC emissions during 2017 (see Fig. S24 and Table S1a).



259 Emissions from gasoline-fueled sources dominate the VOC range in Fig. 3, but diesel-fueled sources, of which there
260 are far fewer in the U.S. dominate the IVOC range. Whereas, sources using both fuels are important for CROC
261 emissions. Mobile source VOCs comprise many functionalities, and aromatics make a substantial contribution. The
262 higher volatility IVOCs have mass associated with aromatics from gasoline sources, but cyclic hydrocarbon
263 compounds contribute to IVOCs across all volatilities, a feature reported by Zhao et al. (2015) We currently lack data
264 to specify CROC functionality across all mobile categories, so we have labeled them alkane-like based on observations
265 of motor vehicle POA emissions (Worton et al., 2014). Improved CROC speciation is needed, especially given the
266 importance of functionality to SOA formation (Lim and Ziemann, 2009; Yee et al., 2013).

267 **3.2 Impact of Filter Artifacts**

268 Transitioning from the Conventional approach to the ROC approach has implications for near-source particle
269 concentrations and prompt SOA production. Figure 4 shows the contributions of mobile categories with results using
270 approaches from previous work (Murphy et al., 2017; Lu et al., 2020). The Conventional approach assumes all OM
271 stays in the particle phase, which has been shown to lead to poor AQM performance (Murphy et al., 2017). The
272 ‘Robinson et al.’ case, which is consistent with CMAQv5.3.2, applies the volatility distribution for a small nonroad
273 diesel engine, where half the OM mass is assumed to be IVOCs adsorbed to filters and is thus volatilized. As seen in
274 Fig. 4, only 25% of the OM persists in the particle after evaporation in the ‘Robinson et al.’ approach. Lu et al. (2020)
275 applied gasoline and diesel-specific volatility profiles parameterized for emissions from in-use vehicles to the entire
276 mobile category, leading to less evaporation of OM than the ‘Robinson et al.’ approach. Lu et al. (2020) also applied
277 a conversion factor of 1.4 to all mobile gasoline-fueled sources to account for missing SVOCs.

278 In the ROC approach here, we apply source-specific adjustment factors (Table S5) and volatility profiles (Table S6)
279 and find similar results for onroad gasoline and nonroad diesel compared to Lu et al. (2020). However, onroad diesel
280 CROC emissions are increased by 60% relative to the CROC emissions from the ‘Lu et al.’ approach, driven by the
281 inclusion of missing SVOCs from clean test conditions for diesel engines with DPFs. Conventional OM emissions
282 from nonroad sources are greater than those from onroad for both gasoline- and diesel-fueled sources. Nonroad
283 gasoline emissions reduced by 36% relative to ‘Lu et al.’ where emission factors are large, and CROC/OM is much
284 less than 1.0 (Table S5), indicating the presence of IVOCs on the filter. Predicted conventional OM emissions from
285 air, rail, and marine sources are also important, and CROC emissions are slightly larger than OM. Across the mobile
286 sector, total CROC emissions increased by 12% relative to OM, and 42% of the CROC emissions are predicted to be
287 in the particle phase at 298 K and $10 \mu\text{g m}^{-3}$ organic aerosol (OA) loading.

288 **3.3 National-Scale Impact on PM, O₃ and HAPs**

289 When aggregated across all mobile sources, total ROC emissions are nearly identical between the Conventional
290 approach and ROC approach (Fig. 5). Total IVOC emissions are represent only 10.2% of total GROC due to the
291 substantial role of VOCs from gasoline sources to ROC emissions in the U.S. The spatial distribution of IVOC and
292 CROC emissions highlight the key role of cities, highways, and shipping lanes (Fig. S26). We calculate the OA
293 potential as the sum of particle-phase mass (calculated at 298 K and $10 \mu\text{g m}^{-3}$) for each species and the SOA yield of
294 the vapor-phase component of each species. Mobile source OA potential has contributions from all ROC volatility



295 classes with 6.8% from LVOCs, 25.4% from SVOCs, 19.1% from IVOCs, and 48.7% from VOCs (Fig. 5). The
296 estimated VOC OA potential is mainly driven by adjusted yields of aromatic VOCs, which are enhanced over previous
297 work due to corrections for vapor wall-losses of single-ring aromatic yields (Zhang et al., 2014). These metrics
298 possibly reflect an upper bound on VOC and IVOC contribution as they apply SOA yields to the precursor emission
299 without consideration of reaction rates, timescales, or competitive losses of precursors and intermediates to deposition.
300 Potential OA relative contributions from air, marine, and rail (12%) and onroad diesel (16%) sources play a larger
301 role in OA potential when emissions are estimated with the ROC approach, while nonroad gasoline and diesel (38%)
302 and onroad gasoline potential OA (34%) decrease (Fig. 6). While aromatic species dominate OA potential in the VOC
303 precursor range, in the IVOC range OA potential has larger contributions from cyclic alkane compounds from onroad
304 diesel sources (Fig. S23). In the LVOC range and below, the ROC approach assumes only alkane-like species;
305 improvements to the SPECIATE database and emissions modeling tools will support increased detail on compound
306 functionality when provided by future studies.

307 VOCs account for 97% of the ozone potential approximated by maximum incremental reactivity (MIR), and the total
308 ozone potential decreases by 8.9% due to the shift in mass from VOC to IVOC. The national-scale source distribution
309 of O₃ potential changes little between the Conventional and ROC approaches (Fig. 6). Ozone potential is dominated
310 by onroad and nonroad gasoline sources in the highest ROC volatility bins, driven by alkane, aromatic, and oxygenated
311 species, as expected (Fig. S23). Among onroad light duty gasoline vehicles, 72% of ROC emissions, 68% of O₃
312 potential, and 79% of OA potential are predicted to come from pre-Tier 2 vehicles, while these vehicles account for
313 19% of the fuel used in 2017 (Fig. S25). Heavy-duty diesel vehicles without particulate filters or selective catalytic
314 reduction systems contribute 87% of ROC emissions, 85% of O₃ potential, and 91% of OA potential while using 31%
315 of the fuel for the heavy-duty diesel onroad category.

316 National-scale HAP emissions changed substantially with updates in VOC speciation and introduction of IVOCs with
317 many species decreasing by nearly 20% or more including toluene (-19%), hexane (-22%), 1,3-butadiene (-34%), and
318 ethyl benzene (-29%) and others increasing substantially including formaldehyde (+22%), acrolein (+20%), and
319 acetaldehyde (+19%) (Fig. S25). These results emphasize the need for more research on HAP emission factors, but
320 we keep them constant for the CMAQ simulations to focus on OA and O₃ changes.

321 **3.4 Air quality model results**

322 Mobile ROC emissions were generated for the year 2017 to be comparable with the EQUATES 2017 emission inputs.
323 Differences between the EQUATES mobile inputs and those for the CMAQ-ROC simulation (Table S9) are consistent
324 with the changes in the 2016 emissions results depicted in Fig. 4. The CMAQ-ROC simulation predicts lower OC
325 concentrations throughout the domain due to elimination of pcSOA. CMAQ-ROC predictions compared well against
326 both O₃ and OC measurements at Air Quality System (AQS) sites in 2017 (Figs. S28, S29 and Table S10). Normalized
327 mean biases for OC improved (in absolute terms and on average) by 11.3% in spring, 4.3% in autumn, and 7.6% in
328 winter. In summer, the OC underprediction increased by 12%. Overprediction in the northeast, Ohio Valley, Upper
329 Midwest, and northwest in winter is consistent with timing and geography of residential wood combustion emissions,
330 which may be overrepresented in both simulations. Root mean square error and correlation coefficient differences



331 between the EQUATES and CMAQ-ROC simulations are small. CMAQ predicts both the annual mean and variability
332 of OC concentrations well at selected U.S. cities (Fig. S34, S35), with the exception of New York City where the
333 model overpredicted OC by more than a factor of 2.

334 The predicted annual population-weighted average OA attributable to mobile sources is $0.26 \mu\text{g m}^{-3}$, or 9% of the OA
335 from all anthropogenic and biogenic sources. Mobile source contributions to POA and SOA are similar on average,
336 with apparent spatial differences (Fig. 7). Average total mobile source OA appears stable between winter and summer
337 seasons (Fig. S30), and this is a result of trade-offs between higher POA concentrations in winter and higher SOA in
338 summer (Figs. S31, S32). In rural areas, model-predicted mobile OA contributions asymptote at 4.5% of total OA,
339 and in some urban areas they can exceed 23% (annual averages; Fig. S33). The ratio of SOA to OA is equal to 70%
340 in rural areas and decreases with increasing population to 20-40%. Diurnal profiles at select cities indicate SOA
341 formation peaks at noon in Los Angeles, Denver, Chicago and New York, but that feature is not reproduced on average
342 at Houston and Raleigh (Figs S34, S35).

343 CMAQ-ROC mobile and VCP IVOC concentrations are enhanced in urban areas with minimal seasonal differences
344 predicted (Figs. S36, S37). Mobile sources are predicted to contribute 20-25% to total IVOCs depending on location
345 and time of year, while VCP sources contribute 59-66% (Fig. S36), although IVOCs from other sources are
346 underrepresented. The composition of ambient IVOCs predicted by CMAQ-ROC and the speciation of IVOC
347 emissions from mobile and VCP emissions are consistent with results from Zhao et al. (Fig. S38). Since ambient
348 IVOC concentration measurements for 2017 are lacking, we extrapolated concentrations to the CalNex campaign in
349 2010 and find acceptable agreement with campaign-average hydrocarbon and oxygenated IVOC observations (section
350 S8, Fig. S39a,b). Extrapolation of CMAQ-ROC SOA to 2010 underpredicts mean CalNex SOA observations by 46%
351 (Fig. S41c,d). Potential explanations include underestimated emissions from other sources (e.g. cooking),
352 mischaracterized chemical processing (e.g. SOA yields), or errors in modeling regional pollution in Southern
353 California (Lu et al., 2020).

354 The U.S. annual GROC emission rate for mobile (2.49 Tg yr^{-1}) is 20% less than that of VCPs (3.09 Tg yr^{-1}), but the
355 mobile IVOC emissions (0.25 Tg yr^{-1}) are only one third those of VCPs (0.77 Tg yr^{-1}). Gas-phase oxidation is
356 responsible for less than half (42% and 44%) of the loss of mobile and VCP SOA-forming GROC, but 88-90% of the
357 IVOC loss (Fig. 8). The annual production and loss of total OA from mobile and VCPs is similar, and loss is distributed
358 evenly across deposition processes and transport out of the model domain. The annual rate of OA production (emission
359 plus chemical production) estimated by CMAQ and normalized to total ROC emissions (i.e. the sum of NMOG plus
360 conventional OM) is $0.16 \text{ g OA (g ROC)}^{-1}$, which is approximately equal to that estimated from the data in Fig. 5. This
361 agreement is surprising considering that the latter calculation does not account for variations in OA partitioning, NO_x
362 effects on SOA yields, or competitive losses from wet scavenging and dry deposition. Seasonal trends for OA, SOA
363 and POA production rates and ambient concentrations normalized to OM and NMOG emissions are tabulated in Table
364 S11 and discussed in section S9. These data may inform simple (e.g. screening) models of the impact of anthropogenic
365 emissions on human exposure.



366 **4. Conclusions**

367 This study implements a detailed source- and species-level procedure for converting conventional OM and NMOG
368 mobile emissions to metrics compatible with the most recent science and speciation developed for atmospheric ROC.
369 Although many AQMs have implemented online or pre-processing emission adjustments to account for these
370 phenomena, (Koo et al., 2014; Murphy et al., 2017) the procedure should be embedded within emission models and
371 databases for several reasons. Most importantly, this detailed approach considers a more diverse population of sources
372 of different ages, fuels, and control technologies that are typically averaged together before they are passed to the
373 AQM. Additionally, the new procedure enables near-explicit speciation of each emission source before mapping to
374 model species used in a particular chemical mechanism. Having a detailed speciation of major emission sources is
375 critical for assessing and revising chemical mechanisms (Pye et al., 2022b). Finally, operationalizing conversions from
376 OM to CROC and NMOG to GROC alleviates AQM users from the burden of interrogating their emissions files to
377 determine whether complex scaling operations are needed. From the broader perspective of facilitating transfer of
378 knowledge between the scientific and regulatory communities, the SPECIATE database is now capable of ingesting
379 speciation profiles with factors aligned with the most recent research studies and has enhanced flexibility to
380 accommodate future updates. Nonetheless, for model applications seeking to scale legacy emission inputs, we provide
381 updated factors normalized to several levels of source aggregation in Table S12 and discuss the uncertainty introduced
382 with this approach in section S10.

383 The 2016 ROC emissions suggest slight decreases to total O₃ formation due to reapportionment of VOC to IVOC in
384 this approach, but 2017 CMAQ-ROC predictions do not meaningfully change when evaluated at AQS sites.
385 Meanwhile, mobile IVOC emissions enhance OA formation by an additional 79 kt yr⁻¹ compared to estimates from
386 the EQUATES configuration (319 kt yr⁻¹). Gaps between total OA measurements and CMAQ-ROC predictions will
387 be addressed through improved modeling of other sources of ROC (e.g. VCPs, wildfires, residential wood combustion,
388 and cooking). Within the mobile sector, results indicate substantial contributions from onroad (46%) and nonroad
389 (41%) gasoline and somewhat less from onroad (5%) and nonroad (3%) diesel air, marine, and rail sources (4.7%;
390 Fig. 6). The vast majority of ROC emissions and impacts are attributable to older (pre-Tier 2 light duty gasoline and
391 non-DPF heavy duty diesel) vehicles and nonroad gasoline engines. Onroad pollution will continue to decrease as
392 these vehicles are phased out, increasing the importance of other mobile source categories and other sources.

393 This study suggests several specific uncertainties pertaining to mobile source emissions need further laboratory and
394 field investigation. Developing complete ROC volatility distributions for specific source classes and control types is
395 critical, especially within the nonroad category where fewer experimental data were available for this study. The
396 CROC/OM factors are uncertain across all mobile sources. Ideally, IVOC and CROC emissions should be sampled
397 by a filter and a broad-spectrum adsorbent tube in series to avoid filter artifacts (Khare et al., 2019). If filter-based
398 methods alone are used to inform organic aerosol emission inventories, then reducing the uncertainty in the
399 relationship between particle emission factor and total CROC will strengthen our confidence in estimating organic
400 aerosol emissions, particularly for lower-emitting technologies. Some CROC/OM ratios derived for this work are
401 between 0.85 and 1.15, indicating a limited role for partitioning bias during source testing in those cases, but many



402 are greater than 1.30, especially the lower-emitting sources. Lastly, more research is needed to determine the extent
403 to which NMOG measurements capture IVOCs (quantified by the IVOC/NMOG or IVOC/GROC ratios). These
404 parameters are especially important to understand for older vehicles and equipment which drive historical and
405 contemporary emissions. We recommend that emissions tests specifically measure and report CROC and GROC to
406 facilitate comparison among datasets and implementation in emission models. Currently, these measurements are
407 beyond the scope of typical regulatory requirements, and future progress requires research beyond regulatory methods.

408 **ASSOCIATED CONTENT**

409 The Supporting Information is available free of charge at
410 Supporting Information 1 (SI-1): Word Document
411 Supporting Information 2 (SI-2): Excel Sheet with Tables
412 The CMAQ model source code used is available via Zenodo (<https://doi.org/10.5281/zenodo.7869142>). The functions
413 to estimate OA and O₃ potential are available at <https://github.com/USEPA/CRACMM>.

414 **ACKNOWLEDGMENT**

415 The authors gratefully acknowledge contributions from U.S. EPA staff including Kristen Foley and George Pouliot
416 who for emissions inputs and Chad Bailey, Michael Hays, and Sergey Napelenok for internal technical reviews. We
417 also acknowledge Yunliang Zhao of the California Air Resources Board for valuable insights and consultation.

418 **AUTHOR INFORMATION**

419 ***Corresponding Author:** Benjamin N. Murphy; Address: Center for Environmental Measurement and Modeling,
420 109 TW Alexander Dr., Durham, NC 27709, USA; Email: murphy.ben@epa.gov; Phone: 919-541-2291

421 **Author Contributions**

422 The manuscript was written and revised through contributions of all authors. All authors have given approval to the
423 final version of the manuscript. DS made contributions to the study primarily when employed by US EPA.

424 **DISCLAIMER**

425 *The views expressed in this article are those of the author(s) and do not necessarily represent the views or the policies*
426 *of the U.S. Environmental Protection Agency*

427 **COMPETING INTERESTS.**

428 *Some authors are members of the editorial board of ACP. The peer-review process was guided by an independent*
429 *editor, and the authors have also no other competing interests to declare.*

430 **REFERENCES**

431 Ahmadov, R., McKeen, S. A., Robinson, A. L., Bahreini, R., Middlebrook, A. M., de Gouw, J. A., Meagher, J.,
432 Hsie, E. Y., Edgerton, E., Shaw, S., and Trainer, M.: A volatility basis set model for summertime secondary
433 organic aerosols over the eastern united states in 2006, *J Geophys Res-Atmos*, 117, 10.1029/2011jd016831,
434 2012.
435



- 436 Appel, K. W., Bash, J. O., Fahey, K. M., Foley, K. M., Gilliam, R. C., Hogrefe, C., Hutzell, W. T., Kang, D.,
437 Mathur, R., Murphy, B. N., Napelenok, S. L., Nolte, C. G., Pleim, J. E., Pouliot, G. A., Pye, H. O. T., Ran,
438 L., Roselle, S. J., Sarwar, G., Schwede, D. B., Sidi, F. I., Spero, T. L., and Wong, D. C.: The community
439 multiscale air quality (cmaq) model versions 5.3 and 5.3.1: System updates and evaluation, *Geosci Model*
440 *Dev.*, 14, 2867-2897, 10.5194/gmd-14-2867-2021, 2021.
- 441 Bergström, R., Denier Van Der Gon, H., Prévôt, A. S., Yttri, K. E., and Simpson, D.: Modelling of organic aerosols
442 over europe (2002–2007) using a volatility basis set (vbs) framework: Application of different assumptions
443 regarding the formation of secondary organic aerosol, *Atmospheric Chemistry and Physics*, 12, 8499-8527,
444 10.5194/acp-12-8499-2012, 2012.
- 445 Bessagnet, B., Allemand, N., Putaud, J. P., Couvidat, F., Andre, J. M., Simpson, D., Pisoni, E., Murphy, B. N., and
446 Thunis, P.: Emissions of carbonaceous particulate matter and ultrafine particles from vehicles-a scientific
447 review in a cross-cutting context of air pollution and climate change, *Appl Sci (Basel)*, 12, 1-52,
448 10.3390/app12073623, 2022.
- 449 Birch, M. and Cary, R.: Elemental carbon-based method for monitoring occupational exposures to particulate diesel
450 exhaust, *Aerosol Science and Technology*, 25, 221-241, 10.1080/02786829608965393, 1996.
- 451 Chang, X., Zhao, B., Zheng, H. T., Wang, S. X., Cai, S. Y., Guo, F. Q., Gui, P., Huang, G. H., Wu, D., Han, L. C.,
452 Xing, J., Man, H. Y., Hu, R. L., Liang, C. R., Xu, Q. C., Qiu, X. H., Ding, D., Liu, K. Y., Han, R.,
453 Robinson, A. L., and Donahue, N. M.: Full-volatility emission framework corrects missing and
454 underestimated secondary organic aerosol sources, *One Earth*, 5, 403-412, 10.1016/j.oneear.2022.03.015,
455 2022.
- 456 Chow, J. C., Watson, J. G., Pritchett, L. C., Pierson, W. R., Frazier, C. A., and Purcell, R. G.: The dri thermal/optical
457 reflectance carbon analysis system: Description, evaluation and applications in us air quality studies,
458 *Atmospheric Environment. Part A. General Topics*, 27, 1185-1201, 10.1016/0960-1686(93)90245-T, 1993.
- 459 Donahue, N. M., Robinson, A. L., and Pandis, S. N.: Atmospheric organic particulate matter: From smoke to
460 secondary organic aerosol, *Atmospheric Environment*, 43, 94-106, 10.1016/j.atmosenv.2008.09.055, 2009.
- 461 Drozd, G. T., Zhao, Y., Saliba, G., Frodin, B., Maddox, C., Oliver Chang, M.-C., Maldonado, H., Sardar, S., Weber,
462 R. J., and Robinson, A. L.: Detailed speciation of intermediate volatility and semivolatile organic
463 compound emissions from gasoline vehicles: Effects of cold-starts and implications for secondary organic
464 aerosol formation, *Environmental science & technology*, 53, 1706-1714, 10.1021/acs.est.8b05600, 2018.
- 465 FAA: Aviation environmental design tool (aedt) version 3e, U.S Department of Transportation <https://aedt.faa.gov/>,
466 2022.
- 467 Foley, K. M., Pouliot, G. A., Eyth, A., Aldridge, M. F., Allen, C., Appel, K. W., Bash, J. O., Beardsley, M., Beidler,
468 J., and Choi, D.: 2002-2017 anthropogenic emissions data for air quality modeling over the united states,
469 *Data in Brief*, 109022, 10.1016/j.dib.2023.109022, 2023.
- 470 Gentner, D. R., Harley, R. A., Miller, A. M., and Goldstein, A. H.: Diurnal and seasonal variability of gasoline-
471 related volatile organic compound emissions in riverside, california, *Environmental science & technology*,
472 43, 4247-4252, 10.1021/es9006228, 2009.
- 473 Gentner, D. R., Isaacman, G., Worton, D. R., Chan, A. W., Dallmann, T. R., Davis, L., Liu, S., Day, D. A., Russell,
474 L. M., Wilson, K. R., Weber, R., Guha, A., Harley, R. A., and Goldstein, A. H.: Elucidating secondary
475 organic aerosol from diesel and gasoline vehicles through detailed characterization of organic carbon
476 emissions, *Proc Natl Acad Sci U S A*, 109, 18318-18323, 10.1073/pnas.1212272109, 2012.
- 477 Gentner, D. R., Jathar, S. H., Gordon, T. D., Bahreini, R., Day, D. A., El Haddad, I., Hayes, P. L., Pieber, S. M.,
478 Platt, S. M., de Gouw, J., Goldstein, A. H., Harley, R. A., Jimenez, J. L., Prevot, A. S., and Robinson, A.
479 L.: Review of urban secondary organic aerosol formation from gasoline and diesel motor vehicle
480 emissions, *Environ Sci Technol*, 51, 1074-1093, 10.1021/acs.est.6b04509, 2017.
- 481 Heald, C. L. and Kroll, J. H.: The fuel of atmospheric chemistry: Toward a complete description of reactive organic
482 carbon, *Sci Adv*, 6, eaay8967, 10.1126/sciadv.aay8967, 2020.
- 483 Huang, C., Hu, Q., Li, Y., Tian, J., Ma, Y., Zhao, Y., Feng, J., An, J., Qiao, L., Wang, H., Jing, S., Huang, D., Lou,
484 S., Zhou, M., Zhu, S., Tao, S., and Li, L.: Intermediate volatility organic compound emissions from a large
485 cargo vessel operated under real-world conditions, *Environ Sci Technol*, 52, 12934-12942,
486 10.1021/acs.est.8b04418, 2018.
- 487 Humes, M. B., Wang, M., Kim, S., Machesky, J. E., Gentner, D. R., Robinson, A. L., Donahue, N. M., and Presto,
488 A. A.: Limited secondary organic aerosol production from acyclic oxygenated volatile chemical products,
489 *Environmental Science & Technology*, 56, 4806-4815, 10.1021/acs.est.1c07354, 2022.



- 490 Jathar, S. H., Woody, M., Pye, H. O. T., Baker, K. R., and Robinson, A. L.: Chemical transport model simulations
491 of organic aerosol in southern california: Model evaluation and gasoline and diesel source contributions,
492 *Atmos Chem Phys*, 17, 4305-4318, 10.5194/acp-17-4305-2017, 2017a.
- 493 Jathar, S. H., Friedman, B., Galang, A. A., Link, M. F., Brophy, P., Volckens, J., Eluri, S., and Farmer, D. K.:
494 Linking load, fuel, and emission controls to photochemical production of secondary organic aerosol from a
495 diesel engine, *Environ Sci Technol*, 51, 1377-1386, 10.1021/acs.est.6b04602, 2017b.
- 496 Jathar, S. H., Sharma, N., Galang, A., Vanderheyden, C., Takhar, M., Chan, A. W. H., Pierce, J. R., and Volckens,
497 J.: Measuring and modeling the primary organic aerosol volatility from a modern non-road diesel engine,
498 *Atmospheric Environment*, 223, 117221, 10.1016/j.atmosenv.2019.117221, 2020.
- 499 Khare, P., Marcotte, A., Sheu, R., Walsh, A. N., Ditto, J. C., and Gentner, D. R.: Advances in offline approaches for
500 trace measurements of complex organic compound mixtures via soft ionization and high-resolution tandem
501 mass spectrometry, *Journal of Chromatography A*, 1598, 163-174, 10.1016/j.chroma.2018.09.014, 2019.
- 502 Kishan, S., Burnette, A., FUncher, S., Sabisch, M., Crews, E., Snow, R., Zmud, M., Santos, R., Bricka, S., Fujita, E.,
503 Campbell, D., and Arnott, P.: Kansas city pm characterization study final report, 2006.
- 504 Koo, B., Knipping, E., and Yarwood, G.: 1.5-dimensional volatility basis set approach for modeling organic aerosol
505 in camx and cmaq, *Atmospheric Environment*, 95, 158-164, 10.1016/j.atmosenv.2014.06.031, 2014.
- 506 Lim, Y. B. and Ziemann, P. J.: Chemistry of secondary organic aerosol formation from oh radical-initiated reactions
507 of linear, branched, and cyclic alkanes in the presence of no x, *Aerosol Science and Technology*, 43, 604-
508 619, 10.1080/02786820902802567, 2009.
- 509 Lipsky, E. M. and Robinson, A. L.: Effects of dilution on fine particle mass and partitioning of semivolatile organics
510 in diesel exhaust and wood smoke, *Environ Sci Technol*, 40, 155-162, 10.1021/es050319p, 2006.
- 511 Lu, Q., Murphy, B. N., Qin, M., Adams, P. J., Zhao, Y., Pye, H. O. T., Efstathiou, C., Allen, C., and Robinson, A.
512 L.: Simulation of organic aerosol formation during the calnex study: Updated mobile emissions and
513 secondary organic aerosol parameterization for intermediate-volatility organic compounds, *Atmos Chem
514 Phys*, 20, 4313-4332, 10.5194/acp-20-4313-2020, 2020.
- 515 Lu, Q. Y., Zhao, Y. L., and Robinson, A. L.: Comprehensive organic emission profiles for gasoline, diesel, and gas-
516 turbine engines including intermediate and semi-volatile organic compound emissions, *Atmospheric
517 Chemistry and Physics*, 18, 17637-17654, 10.5194/acp-18-17637-2018, 2018.
- 518 Lurmann, F., Avol, E., and Gilliland, F.: Emissions reduction policies and recent trends in southern california's
519 ambient air quality, *J Air Waste Manag Assoc*, 65, 324-335, 10.1080/10962247.2014.991856, 2015.
- 520 Manavi, S. E. and Pandis, S. N.: A lumped species approach for the simulation of secondary organic aerosol
521 production from intermediate volatility organic compounds (ivocs): Application to road transport in
522 pmcamx-iv (v1. 0), *Geoscientific Model Development Discussions*, 1-35, 10.5194/gmd-2022-90, 2022.
- 523 May, A. A., Presto, A. A., Hennigan, C. J., Nguyen, N. T., Gordon, T. D., and Robinson, A. L.: Gas-particle
524 partitioning of primary organic aerosol emissions: (1) gasoline vehicle exhaust, *Atmospheric Environment*,
525 77, 128-139, 10.1016/j.atmosenv.2013.04.060, 2013a.
- 526 May, A. A., Presto, A. A., Hennigan, C. J., Nguyen, N. T., Gordon, T. D., and Robinson, A. L.: Gas-particle
527 partitioning of primary organic aerosol emissions: (2) diesel vehicles, *Environ Sci Technol*, 47, 8288-8296,
528 10.1021/es400782j, 2013b.
- 529 May, A. A., Nguyen, N. T., Presto, A. A., Gordon, T. D., Lipsky, E. M., Karve, M., Gutierrez, A., Robertson, W. H.,
530 Zhang, M., Brandow, C., Chang, O., Chen, S. Y., Cicero-Fernandez, P., Dinkins, L., Fuentes, M., Huang,
531 S. M., Ling, R., Long, J., Maddox, C., Massetti, J., McCauley, E., Miguel, A., Na, K., Ong, R., Pang, Y. B.,
532 Rieger, P., Sax, T., Truong, T., Vo, T., Chattopadhyay, S., Maldonado, H., Maricq, M. M., and Robinson,
533 A. L.: Gas- and particle-phase primary emissions from in-use, on-road gasoline and diesel vehicles,
534 *Atmospheric Environment*, 88, 247-260, 10.1016/j.atmosenv.2014.01.046, 2014.
- 535 Morino, Y., Chatani, S., Fujitani, Y., Tanabe, K., Murphy, B. N., Jathar, S. H., Takahashi, K., Sato, K., Kumagai,
536 K., and Saito, S.: Emissions of condensable organic aerosols from stationary combustion sources over
537 japan, *Atmospheric Environment*, 289, 119319, 10.1016/j.atmosenv.2022.119319, 2022.
- 538 Murphy, B. N. and Pandis, S. N.: Simulating the formation of semivolatile primary and secondary organic aerosol in
539 a regional chemical transport model, *Environ Sci Technol*, 43, 4722-4728, 10.1021/es803168a, 2009.
- 540 Murphy, B. N., Donahue, N. M., Robinson, A. L., and Pandis, S. N.: A naming convention for atmospheric organic
541 aerosol, *Atmospheric Chemistry and Physics*, 14, 5825-5839, 10.5194/acp-14-5825-2014, 2014.
- 542 Murphy, B. N., Woody, M. C., Jimenez, J. L., Carlton, A. M. G., Hayes, P. L., Liu, S., Ng, N. L., Russell, L. M.,
543 Setyan, A., Xu, L., Young, J., Zaveri, R. A., Zhang, Q., and Pye, H. O. T.: Semivolatile poa and
544 parameterized total combustion soa in cmaq5.2: Impacts on source strength and partitioning, *Atmos Chem
545 Phys*, 17, 11107-11133, 10.5194/acp-17-11107-2017, 2017.



- 546 Pennington, E. A., Seltzer, K. M., Murphy, B. N., Qin, M., Seinfeld, J. H., and Pye, H. O.: Modeling secondary
547 organic aerosol formation from volatile chemical products, *Atmospheric chemistry and physics*, 21, 18247-
548 18261, 10.5194/acp-21-18247-2021, 2021.
- 549 Pye, H. O. T., Appel, K. W., Seltzer, K. M., Ward-Caviness, C. K., and Murphy, B. N.: Human-health impacts of
550 controlling secondary air pollution precursors, *Environ Sci Technol Lett*, 9, 96-101,
551 10.1021/acs.estlett.1c00798, 2022a.
- 552 Pye, H. O. T., Place, B. K., Murphy, B. N., Seltzer, K. M., and D'Ambro, E. L.: Linking gas, particulate, and toxic
553 endpoints to air emissions in the community regional atmospheric chemistry multiphase mechanism
554 (cracmm) version 1.0 *Atmospheric Chemistry and Physics*, 2022b.
- 555 Pye, H. O. T., Ward-Caviness, C. K., Murphy, B. N., Appel, K. W., and Seltzer, K. M.: Secondary organic aerosol
556 association with cardiorespiratory disease mortality in the united states, *Nat Commun*, 12, 7215,
557 10.1038/s41467-021-27484-1, 2021.
- 558 Reff, A., Bhave, P. V., Simon, H., Pace, T. G., Pouliot, G. A., Mobley, J. D., and Houyoux, M.: Emissions inventory
559 of pm2.5 trace elements across the united states, *Environ Sci Technol*, 43, 5790-5796, 10.1021/es802930x,
560 2009.
- 561 Robinson, A. L., Grieshop, A. P., Donahue, N. M., and Hunt, S. W.: Updating the conceptual model for fine particle
562 mass emissions from combustion systems allen I. Robinson, *Journal of the Air & Waste Management*
563 *Association*, 60, 1204-1222, 10.3155/1047-3289.60.10.1204, 2010.
- 564 Robinson, A. L., Donahue, N. M., Shrivastava, M. K., Weitkamp, E. A., Sage, A. M., Grieshop, A. P., Lane, T. E.,
565 Pierce, J. R., and Pandis, S. N.: Rethinking organic aerosols: Semivolatile emissions and photochemical
566 aging, *Science*, 315, 1259-1262, 10.1126/science.1133061, 2007.
- 567 Safieddine, S. A., Heald, C. L., and Henderson, B. H.: The global nonmethane reactive organic carbon budget: A
568 modeling perspective, *Geophysical Research Letters*, 44, 3897-3906, 10.1002/2017gl072602, 2017.
- 569 Seltzer, K. M., Pennington, E., Rao, V., Murphy, B. N., Strum, M., Isaacs, K. K., and Pye, H. O. T.: Reactive
570 organic carbon emissions from volatile chemical products, *Atmos Chem Phys*, 21, 5079-5100,
571 10.5194/acp-21-5079-2021, 2021.
- 572 Shrivastava, M., Fast, J., Easter, R., Gustafson, W. I., Zaveri, R. A., Jimenez, J. L., Saide, P., and Hodzic, A.:
573 Modeling organic aerosols in a megacity: Comparison of simple and complex representations of the
574 volatility basis set approach, *Atmospheric Chemistry and Physics*, 11, 6639-6662, 10.5194/acp-11-6639-
575 2011, 2011.
- 576 Simon, H., Bhave, P. V., Swall, J. L., Frank, N. H., and Malm, W. C.: Determining the spatial and seasonal
577 variability in om/oc ratios across the us using multiple regression, *Atmospheric Chemistry and Physics*, 11,
578 2933-2949, 10.5194/acp-11-2933-2011, 2011.
- 579 Tessum, C. W., Paoletta, D. A., Chambliss, S. E., Apte, J. S., Hill, J. D., and Marshall, J. D.: Pm2.5 pollutants
580 disproportionately and systemically affect people of color in the united states, *Sci Adv*, 7, eabf4491,
581 10.1126/sciadv.abf4491, 2021.
- 582 Tkacik, D. S., Presto, A. A., Donahue, N. M., and Robinson, A. L.: Secondary organic aerosol formation from
583 intermediate-volatility organic compounds: Cyclic, linear, and branched alkanes, *Environ Sci Technol*, 46,
584 8773-8781, 10.1021/es301112c, 2012.
- 585 U.S. EPA: Integrated science assessment (isa) for particulate matter (final report, dec 2019), 2019.
- 586 U.S. EPA: Speciatev5.1, U.S. EPA <https://www.epa.gov/air-emissions-modeling/speciate>, 2020a.
- 587 U.S. EPA: Motor vehicle emission simulator: Moves3, Office of Transportation and Air Quality, U.S. EPA
588 <https://www.epa.gov/moves>, 2020b.
- 589 U.S. EPA: Integrated science assessment (isa) for ozone and related photochemical oxidants (final report, apr 2020),
590 2020c.
- 591 U.S. EPA: Community multiscale air quality (cmaq) model v5.3.2, Office of Research and Development, U.S. EPA
592 <https://github.com/USEPA/CMAQ/tree/5.3.2>, 2021.
- 593 U.S. EPA: Technical support document (tsd) preparation of emissions inventories for the 2017 north american
594 emissions modeling platform, 2022a.
- 595 U.S. EPA: Engine testing procedures. Cfr, part 1065, title 40, 2022b.
- 596 U.S. EPA: Equates: Epa's air quality time series project, U.S. EPA [dataset], 2022c.
- 597 Winkler, S., Anderson, J., Garza, L., Ruona, W., Vogt, R., and Wallington, T.: Vehicle criteria pollutant (pm, nox,
598 co, hcs) emissions: How low should we go?, *Npj Climate and atmospheric science*, 1, 1-5, 10.1038/s41612-
599 018-0037-5, 2018.



- 600 Woody, M. C., West, J. J., Jathar, S. H., Robinson, A. L., and Arunachalam, S.: Estimates of non-traditional
601 secondary organic aerosols from aircraft svoc and ivoc emissions using cmaq, *Atmospheric Chemistry and*
602 *Physics*, 15, 6929-6942, 10.5194/acp-15-6929-2015, 2015.
- 603 Woody, M. C., Baker, K. R., Hayes, P. L., Jimenez, J. L., Koo, B., and Pye, H. O.: Understanding sources of organic
604 aerosol during calnex-2010 using the cmaq-vbs, *Atmospheric Chemistry and Physics*, 16, 4081-4100,
605 10.5194/acp-16-4081-2016, 2016.
- 606 Worton, D. R., Isaacman, G., Gentner, D. R., Dallmann, T. R., Chan, A. W., Ruehl, C., Kirchstetter, T. W., Wilson,
607 K. R., Harley, R. A., and Goldstein, A. H.: Lubricating oil dominates primary organic aerosol emissions
608 from motor vehicles, *Environmental science & technology*, 48, 3698-3706, 10.1021/es405375j, 2014.
- 609 Yee, L., Craven, J., Loza, C., Schilling, K., Ng, N., Canagaratna, M., Ziemann, P., Flagan, R., and Seinfeld, J.:
610 Effect of chemical structure on secondary organic aerosol formation from c 12 alkanes, *Atmospheric*
611 *Chemistry and Physics*, 13, 11121-11140, 10.5194/acp-13-11121-2013, 2013.
- 612 Zhang, X., Cappa, C. D., Jathar, S. H., McVay, R. C., Ensberg, J. J., Kleeman, M. J., and Seinfeld, J. H.: Influence
613 of vapor wall loss in laboratory chambers on yields of secondary organic aerosol, *Proceedings of the*
614 *National Academy of Sciences*, 111, 5802-5807, 10.1073/pnas.1404727111, 2014.
- 615 Zhao, B., Wang, S., Donahue, N. M., Jathar, S. H., Huang, X., Wu, W., Hao, J., and Robinson, A. L.: Quantifying
616 the effect of organic aerosol aging and intermediate-volatility emissions on regional-scale aerosol pollution
617 in china, *Sci Rep*, 6, 28815, 10.1038/srep28815, 2016a.
- 618 Zhao, Y., Tkacik, D. S., May, A. A., Donahue, N. M., and Robinson, A. L.: Mobile sources are still an important
619 source of secondary organic aerosol and fine particulate matter in the los angeles region, *Environmental*
620 *Science & Technology*, 56, 15328-15336, 10.1021/acs.est.2c03317, 2022.
- 621 Zhao, Y., Nguyen, N. T., Presto, A. A., Hennigan, C. J., May, A. A., and Robinson, A. L.: Intermediate volatility
622 organic compound emissions from on-road diesel vehicles: Chemical composition, emission factors, and
623 estimated secondary organic aerosol production, *Environ Sci Technol*, 49, 11516-11526,
624 10.1021/acs.est.5b02841, 2015.
- 625 Zhao, Y., Nguyen, N. T., Presto, A. A., Hennigan, C. J., May, A. A., and Robinson, A. L.: Intermediate volatility
626 organic compound emissions from on-road gasoline vehicles and small off-road gasoline engines, *Environ*
627 *Sci Technol*, 50, 4554-4563, 10.1021/acs.est.5b06247, 2016b.
- 628 Zhao, Y., Hennigan, C. J., May, A. A., Tkacik, D. S., de Gouw, J. A., Gilman, J. B., Kuster, W. C., Borbon, A., and
629 Robinson, A. L.: Intermediate-volatility organic compounds: A large source of secondary organic aerosol,
630 *Environ Sci Technol*, 48, 13743-13750, 10.1021/es5035188, 2014.

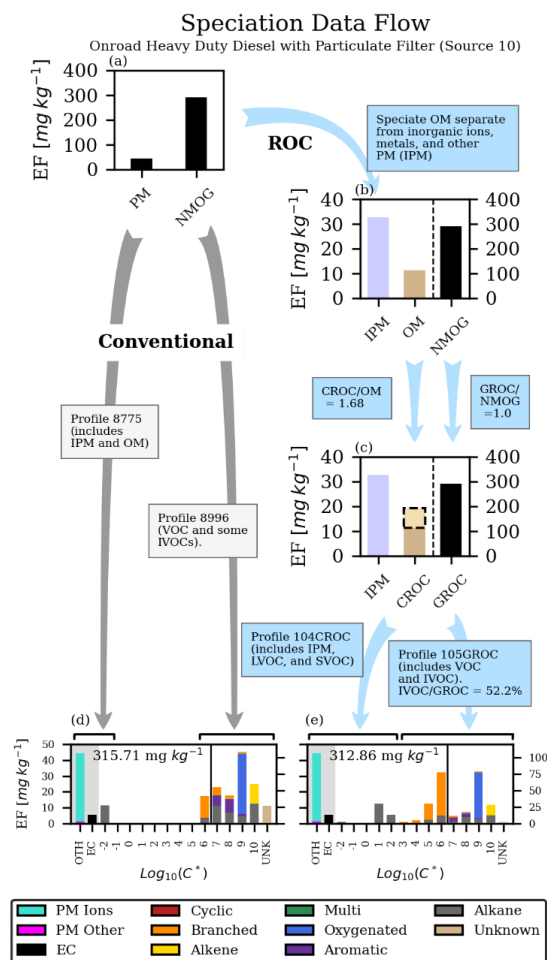
631



632 **Table 1.** Definitions of key terms.

Acronym	Definition
OM	Organic matter component of primary particle emissions as measured on a filter.
NMOG	Non-methane organic gas emissions
POA	Primary organic aerosol. Particle-phase emissions after equilibrium is reached with ambient conditions.
OA	Particle-phase organic material at ambient conditions.
LVOC	Low-volatility organic compounds ($C^* \leq 0.32 \mu\text{g m}^{-3}$).
SVOC	Semivolatile organic compounds ($0.32 < C^* \leq 320 \mu\text{g m}^{-3}$).
IVOC	Intermediate volatility organic compounds ($320 < C^* \leq 3.2 \times 10^6 \mu\text{g m}^{-3}$).
VOC	Volatile organic compounds ($3.2 \times 10^6 \mu\text{g m}^{-3} < C^*$).
CROC	Condensable reactive organic carbon: particle- and gas-phase LVOC + SVOC. Carbon and noncarbon mass are included.
GROC	Gaseous reactive organic carbon: particle- and gas-phase IVOC + VOC. Carbon and noncarbon mass are included.
ROC	Reactive organic carbon – all particle and gas organic compounds mass except methane. Carbon and noncarbon mass are included.

633
634



635

636 **Figure 1.** Depiction of calculation steps for the Conventional and ROC approaches to speciation of PM and NMOG
 637 emissions. Panel (a) shows the reported fuel-based emission factors based on MOVES predictions for 2016. Panel
 638 (b) shows the inorganic ions, metals and other nonorganic matter (IPM) separated from organic matter (OM). The
 639 beige area inside the dashed box in panel (c) indicates emissions that are added in the conversion of OM to CROC to
 640 account for underrepresented SVOCs from the filter measurement. Panels (d) and (e) show the comprehensive
 641 emission factors for the Conventional and ROC approaches, respectively, with data arranged by volatility while
 642 indicating non-organic PM emissions as well. In panels (d) and (e), bars to the left and right of the vertical line at
 643 $\text{Log}_{10}(\text{C}^*) = 6.5$ are quantified by the left and right y axes, respectively. The number within panels (d) and (e)
 644 indicates the total ROC emission factor excluding EC and Other PM for onroad heavy-duty diesel sources. ‘Alkane’
 645 refers to only linear alkanes, while ‘cyclic’ and ‘branched’ are cyclic alkanes and branched alkanes. ‘Multi’

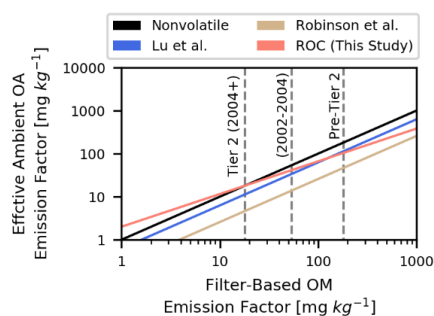


646 indicates multifunctional organics. The bars in the gray shaded regions are not included in the organic volatility
647 distribution but are included in the CROC-compatible SPECIATE profiles (e.g. 104CROC).

648

649

650

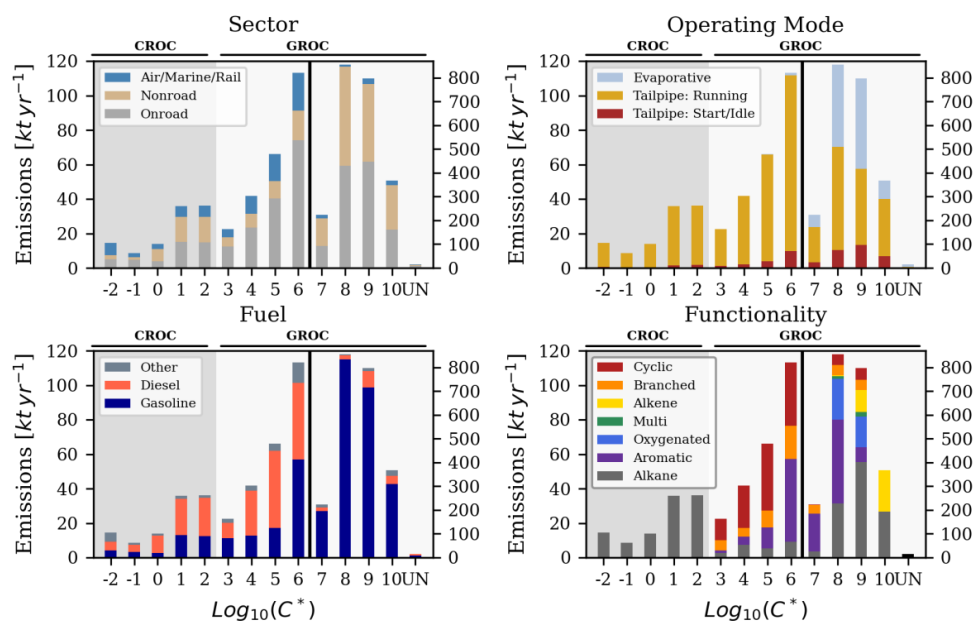


651

652 **Figure 2.** Effective ambient primary organic aerosol emission factor estimated at 298 K and $10 \mu\text{g m}^{-3}$ as a function
653 of the OM emission factor for onroad gasoline-fueled vehicles.

654

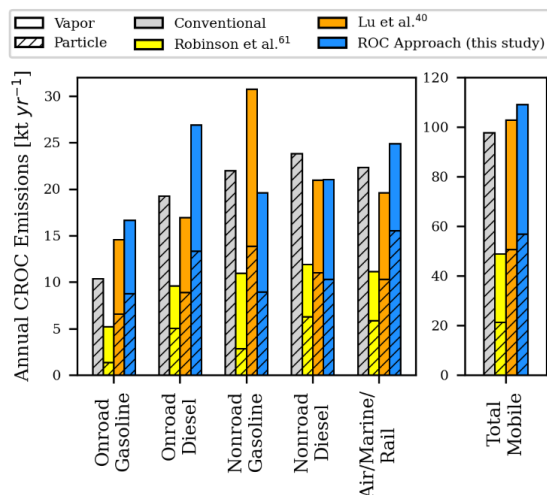
655



656

657 **Figure 3.** Volatility-resolved mobile source ROC emissions for the contiguous U.S. during 2016 stratified along
 658 several dimensions including category (top-left), operating mode (top-right), fuel (bottom-left), and
 659 chemical
 660 functionality (bottom-right). The ‘multi’ functionality series corresponds to compounds that are both oxygenated and
 661 have double carbon bonds. Bins to the left of the solid black line are quantified by the left y axis and those to the right
 662 by the right y axis. The unknown emissions (UN) are not assigned to a volatility bin and do not contribute to OA or
 O₃ formation.

663



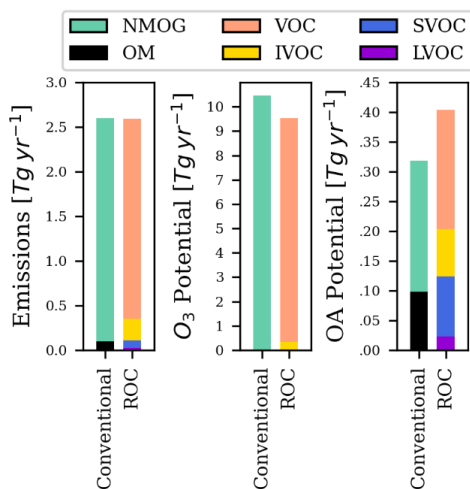
664

665 **Figure 4.** Bottom-up predictions of 2016 annual mobile CROC (i.e. SVOC, LVOC, and lower volatility compound)
 666 emissions classified by category, model approach, and equilibrium phase distribution. The full height of each bar
 667 corresponds to total CROC emissions. Gas-particle partitioning is calculated for atmospherically relevant conditions
 668 at 298 K and organic aerosol loading of 10 $\mu\text{g m}^{-3}$.

669

670

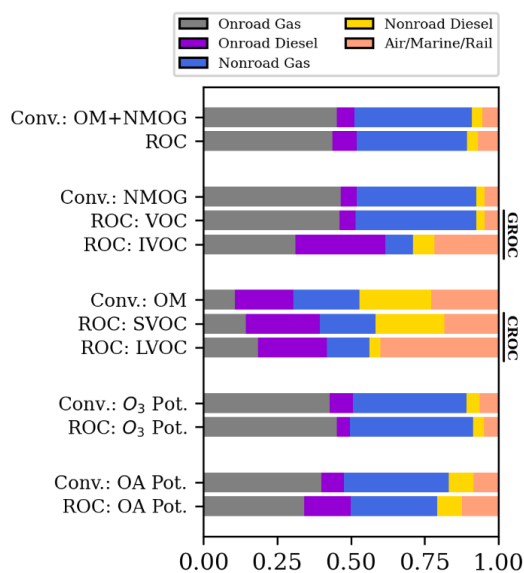
671



672

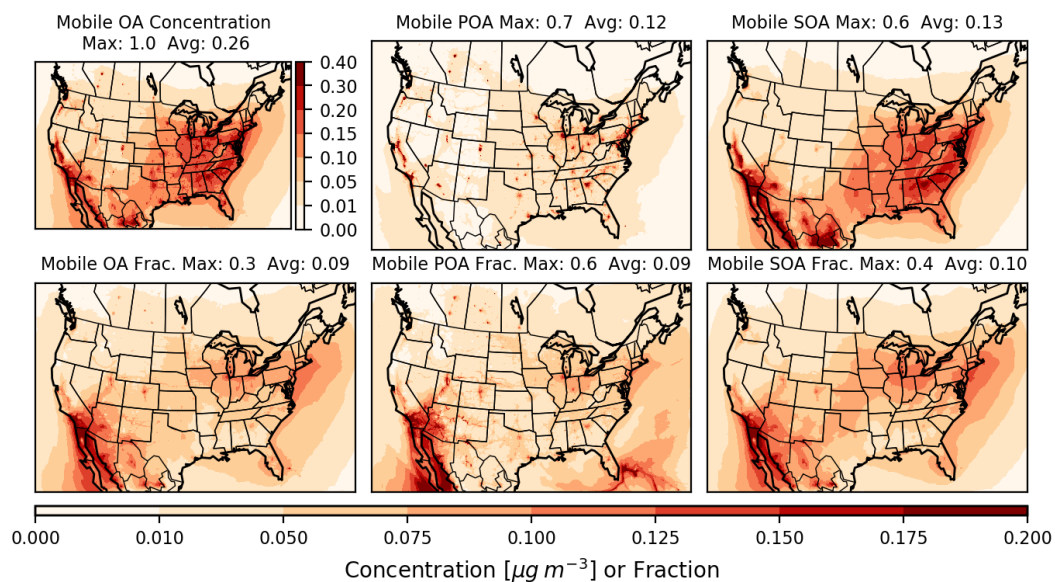
673 **Figure 5.** Total U. S. mobile source emissions for 2016 with aggregate O₃ and OA potential calculated at the species
 674 level.

675



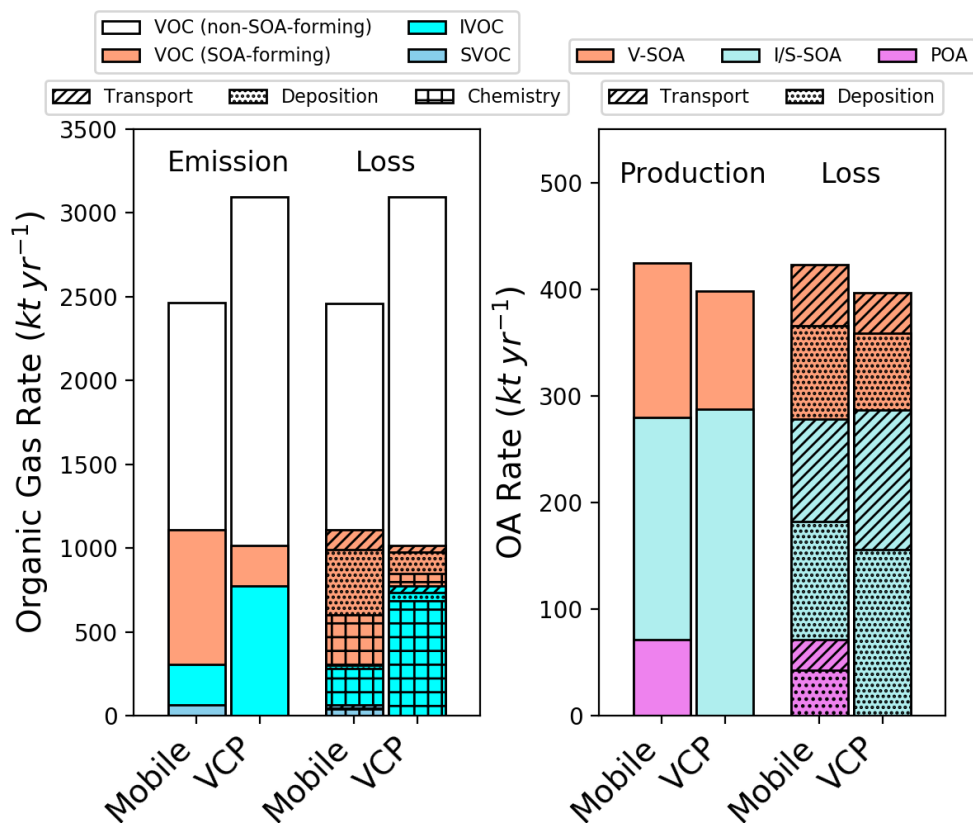
676
677
678

Figure 6. Mobile sector contributions to ROC classes and derived quantities like O₃ and OA potential. Values are presented for the Conventional and ROC-based approaches.



679

680 **Figure 7.** Annual average concentration (top row) of total OA (left), POA (center), and SOA (right) from mobile
681 sources predicted by CMAQ for 2017 with the ROC mobile emission inventory. The fractional contribution of mobile
682 sources to the total of each pollutant category from all sources are on the bottom row. In all panel subtitles, 'Max'
683 refers to the spatial maximum of the annual average spatial field, while 'Avg' refers to the population-weighted
684 average of the annual average spatial field.



685
686
687
688
689

Figure 8. Domain-wide predicted budget of (left) mobile and volatile chemical product (VCP) gas-phase emissions and loss due to chemistry, deposition, or transport and (right) OA production and losses for 2017. In the left plot, loss terms are only depicted for categories of compounds that lead to organic particle formation.